# CHAPTER 14

## APPLICATION OF A NESTED NUMERICAL MODEL TO IDEALISED RECTANGULAR HARBOURS

by

Roger A. Falconer[1] and Lida Mardapitta-Hadjipandeli[2]

Abstract

The paper gives details of a two-dimensional depth averaged nested numerical model and its application to a range of idealised rectangular harbours, having a constant plan cross-sectional area and varying length to breadth ratios. The main aims of the study have been to investigate the problems associated with nested numerical modelling and to apply this modelling approach to assess the influence of the shape of a harbour on its natural tidal flushing efficiency and mixing characteristics.

### Introduction

In recent years there has been an increasing awareness of the tidal exchange characteristics and flushing efficiencies of ports, harbours and narrow entranced coastal basins. This incresed awareness can be attributed to a number of factors and, in particular, is partly attributable to the occurrence of poor water quality characteristics within both natural and man-made harbours and coastal basins. The main problems giving rise to poor water quality characteristics in coastal basins include such phenomena as:- low dissolved oxygen, eutrophication and low exchange rates and flushing efficiencies. The greater public concern and awareness of deteriorating water quality characteristics has partly arisen as a result of increased recreation and has led to many countries now establishing guidelines as to acceptable water quality standards within such coastal basins.

In attempting to minimise the occurrence of such phenomena as low dissolved oxygen and low tidal exchange rates, there are insufficient engineering design guidelines available to the coastal engineer faced with the task of designing a new harbour or modifying an existing coastal basin. For example, little knowledge exists in the technical literature as to:- (i) the optimum shape of harbours for maximum flushing efficiency, (ii) the ideal entrance configuration, (iii) the optimum depth for maximum flushing and minimum dredging requirements, and (iv) the effects of longshore currents on the basin's internal flow structure and exchange characteristics. Furthermore, the use of traditional physical model studies to obtain related design guidelines concerning tidal flushing and exchange characteristics for harbours is of limited

1. Lecturer in Civil Engineering, University of Birmingham, Birmingham, England.

2. Formerly Research Student, Department of Civil Engineering, University of Birmingham, England.

value, in view of the scaling problems associated with recirculating free surface flow models, i.e. Reynolds number effects. These scaling problems are particularly prevalent in harbours where the dimensions of the plan-form area, the narrow entrance width and the tidal range are such that tidal eddies occur within the basin on the flood tide.

In view of the growing concern about the water quality characteristics within narrow entranced coastal basins, such as harbours, and the problems associated with related physical model studies, there has also been an increasing use made of mathematical models for such studies e.g. Falconer (1,2). These mathematical model studies have either been undertaken for site specific studies or have been associated with related research programmes, such as:- (i) fluid mechanics and turbulence modelling, (ii) cohesive sediments and mud transport modelling, (iii) aspects of ecological, biological and chemical reaction modelling, e.g. the nitrification cycle, (iv) numerical methods, e.g. discontinuity modelling related to sewage effluent outfalls, and (v) field data acquisition and interpretation.

In earlier work reported by Falconer (1,3), a single grid-size mathematical model study was described wherein the model was specifically developed to predict the two-dimensional tide induced recirculatory velocity fields and solute transport distributions in harbours and narrow entranced coastal basins. Although reasonably encouraging agreement was obtained between the mathematical and physical model velocity and solute transport fields, at the same scale, no counter-rotating gyres - or tidal eddies - were predicted in the numerical model simulations and the dominant tidal eddy was always observed to be distinctly weaker in the numerical model predictions. The main cause of these discrepancies was attributed to the imprecise description of the velocity field at the harbour entrance and hence the main objective of this study was to develop a nested two-dimensional flow and solute transport model, with the aim of describing the velocity distribution across the harbour entrance more accurately. The model, which only required a marginal increase in the computational effort relative to the single grid-size model, was then applied to the rectangular harbours studied in an earlier research programme, by Falconer (1,3). The model was also used to investigate the effects of varying the harbour shape, entrance conditions and tidal range, with a view to establishing some fundamental engineering guidelines relating to the water quality aspects of rectangular harbours. The model included a refined turbulence model incorporating both free shear layer and bed generated turbulence, with simulations being undertaken at both prototype and physical model scales. Further physical model tests were undertaken to extend previous findings by Jiang and Falconer (4,5), and experimentally measured and numerically predicted velocity fields and exchange coefficients were compared for the physical model scale dimensions.

## Governing Differential Equations

In determining the velocity and solute transport fields from the mathematical model, the depth averaged velocity components in the horizontal plane and the spatial solute distributions were obtained from the depth integrated equations of continuity, momentum - in both x and y directions in the horizontal plane - and the solute transport or

advective-diffusion equation. The full derivation of these equations is given by Falconer (6), with the equations of mass and momentum conservation being respectively given as:-

$$\frac{\partial \eta}{\partial t} + \frac{\partial UH}{\partial x} + \frac{\partial VH}{\partial y} = 0 \qquad \text{.... (1)}$$

$$\frac{\partial UH}{\partial t} + \beta\left[\frac{\partial U^2H}{\partial x} + \frac{\partial UVH}{\partial y}\right] - fVH + gH\frac{\partial \eta}{\partial x} + \frac{\tau_{bx}}{\rho} - \frac{1}{\rho}\left[\frac{\partial H\sigma_{xx}}{\partial x} + \frac{\partial H\tau_{xy}}{\partial y}\right] = 0 \qquad \text{.... (2)}$$

$$\frac{\partial VH}{\partial t} + \beta\left[\frac{\partial UVH}{\partial x} + \frac{\partial V^2H}{\partial y}\right] + fUH + gH\frac{\partial \eta}{\partial y} + \frac{\tau_{by}}{\rho} - \frac{1}{\rho}\left[\frac{H\tau_{yx}}{\partial x} + \frac{H\sigma_{yy}}{\partial y}\right] = 0 \qquad \text{.... (3)}$$

where $\eta$ = water surface elevation above datum (e.g. MWL), t = time, U, V = depth mean velocity components in x,y directions, H = total depth of flow, $\beta$ = momentum correction factor for non-uniform vertical velocity profile, f = Coriolis parameter, g = gravitational acceleration, $\tau_{bx}$, $\tau_{by}$ = bed shear stress components in x,y directions, $\rho$ = fluid density and $\sigma_{xx}$, $\tau_{xy}$, $\tau_{yx}$, $\sigma_{yy}$ = Reynolds stress components in x,y directions.

For the bed shear stress components, the traditional quadratic friction law was used, giving (see Dronkers (7)):-

$$\tau_{bx} = \frac{\rho g U\bar{V}}{c^2} \quad \text{and} \quad \tau_{by} = \frac{\rho g V\bar{V}}{c^2} \qquad \text{.... (4)}$$

where $\bar{V}$ = depth mean fluid speed and C = Chezy roughness coefficient - evaluated in the numerical model from the Colebrook-White equation, given as:-

$$C = \frac{\sqrt{8g}}{\sqrt{f}} = -2\sqrt{8g}\,\log_{10}\left[\frac{k_s}{12R} + \frac{2.5}{Re\sqrt{f}}\right] \qquad \text{.... (5)}$$

where f = Darcy friction factor, $k_s$ = length parameter characteristic of bed roughness, R = hydraulic radius, Re = Reynolds number = $4UR\nu^{-1}$ where $\nu$ = kinematic viscosity of fluid.

For the Reynolds stresses, the assumption was made that the direct stresses $\sigma_{xx}$ and $\sigma_{yy}$, were generally small in comparison with the lateral shear stress, $\tau_{xy}$ and $\tau_{yx}$, see Kuipers and Vreugdenhil(8) and, in the mixing zone, the lateral shear stresses were subdivided into two components. These components included turbulent shear contributions arising from free shear layer and bed generated turbulence and can be

summarised for the x-direction as follows:-

$$\tau_{xy} = \rho \left[ \frac{U_1^2}{2\sqrt{2\pi}R} e^{-R/2(y^1/x^1)^2} + \frac{0.16\sqrt{g}\,\bar{V}H}{C} \frac{\partial U}{\partial y} \right] \quad \ldots. \quad (6)$$

where $U^1$ = free stream velocity, R = experimental constant and $x^1$, $y^1$ = co-ordinate axes for the mixing layer. This empirical shear stress distribution is based on the assumption of a Gaussian lateral velocity distribution in the horizontal plane and a logarithmic velocity distribution in the vertical plane. Full details of the derivation of equation (6) are given by Falconer, Wolanski and Mardapitta-Hadjipandeli (9) and Falconer and Mardapitta-Hadjipandeli (10).

The depth integrated advective-diffusion equation was attached to the hydrodynamic model, thereby enabling the transport of a conservative tracer S to be evaluated accordingly:-

$$\frac{\partial SH}{\partial t} + \left[ \frac{\partial SUH}{\partial x} + \frac{\partial SVH}{\partial y} \right] = \frac{\partial}{\partial x} \left[ HD_{xx} \frac{\partial s}{\partial x} + HD_{xy} \frac{\partial s}{\partial y} \right]$$

$$+ \frac{\partial}{\partial y} \left[ HD_{yx} \frac{\partial s}{\partial x} + HD_{yy} \frac{\partial s}{\partial y} \right] \quad \ldots. \quad (7)$$

where $D_{xx}$, $D_{xy}$, $D_{yx}$, $D_{yy}$ = depth mean longitudinal dispersion and turbulent diffusion tensor coefficients in x,y direction, as given by Fischer (11).

Mathematical Model Details

In numerically solving equations (1), (2), (3) and (7) an alternating direction implicit finite difference model was used, including a traditional space staggered grid scheme (see Falconer (2,3)). The difference equations were fully centred in time and space and the advective accelerations and diffusion terms were centred by a single iteration procedure (see Mardapitta-Hadjipandeli(12)). The model had no stability constraints, although it was established that the accuracy of the scheme deteriorated when the Courant number exceeded about eight, i.e. for accuracy:-

$$\Delta t \sqrt{gH}\, \Delta x^{-1} \leq 8 \quad \ldots. \quad (8)$$

where $\Delta t$ = time step and $\Delta x$ = grid spacing.

In the model, particular attention was given to the treatment of the advective accelerations, with these terms being expressed in a conservative form in both the differential and difference equations. This conservative representation of these terms allowed a more accurate simulation of the jet type flow field, associated with the flood tide flow past the narrow harbour entrance. In addition, the cross product advective accelerations were expressed in a modified form of the marker and cell technique, see Falconer et al (9), thereby allowing the momentum flux to be evaluated nearer to its position of

origin and the introduction of sufficient artificial diffusion to eliminate grid scale oscillations.

For the treatment of discontinuities, arising as the tracer contaminated fluid was advected into the region of non-contaminated fluid, sufficient artificial diffusion was introduced into the scheme to avoid the occurrence of negative concentration values. However, other than in the immediate vicinity of the discontinuity, the degree of artificial diffusion introduced into the scheme was negligible. This scheme was similar to that first outlined by Leendertse (13) and is described in more detail in Falconer (14).

Model Application

In extending work undertaken previously by Falconer et al (1)-(5), the physical and mathematical model studies were applied to idealised prototype rectangular harbours, having a flat bed, vertical sides and an asymmetric entrance. The idealised prototype harbour was assumed to have a constant plan-form area of $0.16km^2$, a mean depth of 6.0m, an entrance width of 100m, a tidal range of 5.0m and a variable length to breadth ratio - varying from 0.38 to 4.0. Each harbour shape considered was assumed to be initially contaminated uniformly within the basin by a conservative tracer of concentration 10ppm. The range of harbour shapes considered are illustrated schematically in Fig.1, which gives an illustration of the laboratory tidal tank and the harbour configuration.

For the physical model studies, the basin was modelled using a distorted Froude scale model, with horizontal and vertical length scales of 1:500 and 1:50 respectively. The resulting scaled laboratory model harbours had a plan-form area of $0.64m^2$, a mean depth of 120mm and an entrance width of 100mm. Likewise, for dynamic similarity, the corresponding velocity and time scales were 1:7.07 and 1:70.7 respectively, resulting in a model tidal period of 10.52 minutes and a range of 100mm.

In undertaking the laboratory model tests, the model harbour walls were first adjusted to give the required length to breadth ratio, for the constant plan-form area of $0.64m^2$. The overflow weir was set at the low tide level and the tidal tank was filled and the inflow rate adjusted to ensure a continuous flow over the weir for the whole model tide. After any initial circulation engendered within the basin had been dissipated, the harbour entrance was temporarily sealed and 75ml of Rhodamine B, of concentration 7.5mg/ℓ, was thoroughly mixed with the enclosed harbour fluid. The spatially averaged initial concentration was then determined from twelve evenly distributed sampling points. The temporary barrier across the harbour entrance was then removed and the tidal generator was run for three tides, after which time the generator was stopped and the temporary barrier simultaneously replaced. The spatially averaged final concentration was then determined as before and the exchange coefficient was evaluated as defined by the following equation (see Nece and Richey (15)):-

$$E = 1 - (Co/Ci)^{1/i} \qquad \text{.... (9)}$$

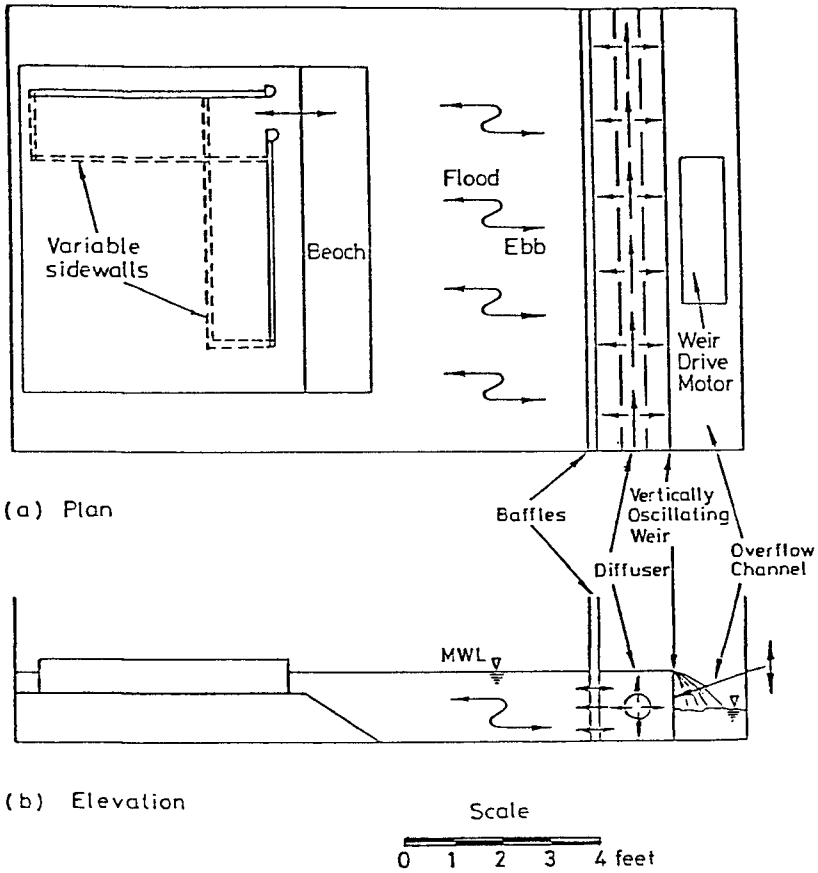


FIG.1 Details of Laboratory Tidal Tank and Harbour Configuration

where E = average per cycle exchange coefficient, Co = initial spatial average concentration, Ci = final spatial average concentration after i tidal cycles.

After the exchange coefficient had been determined, the depth mean velocity field was estimated at mean water level - for both the ebb and flood tide - using weighted drinking straws as drogues. The depth mean velocities were estimated as closely as possible at the intersecting points on a cartesian grid, which coincided with every other grid point of the mathematical model. The complete set of results for the tracer studies and velocity fields are given in Mardapitta-Hadjipandeli (12), with earlier results being given by Falconer et al (1)-(5).

For the mathematical model studies, a one-way interaction nested model was used. One-way interaction models involve the initial computation of the overall coarse-grid model which, in turn, provides the boundary conditions for the independent computation of the small-sized fine-grid model. The alternative two-way interaction models require the simultaneous computation of both grids, thus enabling the regions of different spacings to be dynamically inter-linked. The latter method therefore allows the response of the coarse-grid domain to small-scale processes occurring within the fine grid to be taken into account, giving rise to more coherent results over the computational domain. However, the dynamic coupling of the nested grid requires a more complex computational code. On the contrary, in one-way interaction models it is inherently assumed that the large scale motion of the coarse grid determines the small scale motion in the fine grid, without being affected by small scale processes occurring within the fine grid.

The overall coarse-grid domain for the rectangular harbour model studies was chosen to cover the whole plan-form area of the tidal tank and consisted of 27 x 34 grid points, of uniform grid spacing of 100mm, and with the tidal tank bathymetry being as depicted in Fig.2. At the open boundary, water elevations were presecribed according to a sine wave of the form:-

$$\eta = a \sin(\omega t + \phi) \qquad \ldots\ldots (10)$$

where a = amplitude, $\omega$ = tidal frequency and $\phi$ = phase angle governing the initial conditions. Since the tidal flow entered and exited the tidal tank uniformly across the oscillatory weir and in a direction normal to the open boundary, the advective accelerations were omitted along the open boundary and the tangential velocities were equated to zero. At the closed boundaries the no-slip boundary condition was implemented. A timestep of 0.84s was used in the model, giving rise to a maximum Courant number of about 9.0.

The domain of the fine grid model covered the plan-form area of the model and extended beyond the harbour entrance, as illustrated by the shaded region in Fig.2. The open boundaries of the fine-grid model were located well beyond the harbour entrance, so that small scale inaccuracies at the fine-grid open boundaries did not disturb the internal flow field predictions. The ratio of the grid scales between the coarse and fine grids in such models is arbitrary, although in practice

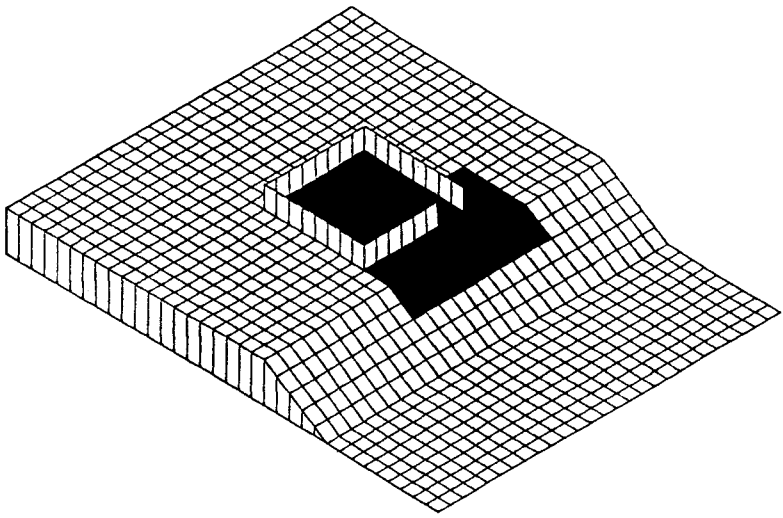

FIG.2 Isoparametric Projection of Tidal Tank Bathymetry Showing Extent of Nested Grid Domain

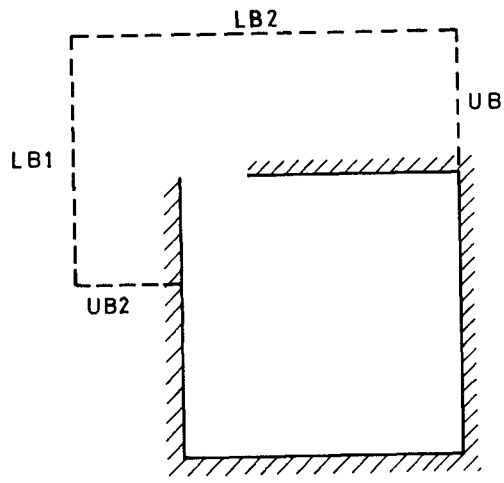


FIG.3 Schematic Illustration of Fine-Grid Open Boundaries

it has been suggested that the ratio should be kept below about 5 (see Thabet et al (16)). In this study the ratio of both the grid and time scales between the two nested grids was chosen to be 3, giving rise to a Courant number of about 9 in both grids. The decrease in the grid size and, as a consequence, in the timestep of the fine-grid model required both the time and space interpolation of the Coarse-grid model predictions in order to provide proper boundary conditions at the appropriate points along the fine-grid model boundaries. In the interpolation process, linear variations were assumed for the velocities and elevations, in both time and space.

Concerning the open boundary conditions of the fine-grid model, no guidelines were available as to the most suitable representation. Tests were therefore undertaken to determine the most appropriate combination of the open boundary conditions for this particular case study. The following combinations of open boundary conditions were tested at the four open boundaries of the fine-grid model (see Fig.3) for the square harbour configuration:-

(a) Water elevations and tangential velocity components along the lower boundaries, LB1 and LB2, and normal and tangential velocity components at the upper boundaries, UB1 and UB2.

(b) Normal and tangential velocity components at the lower boundaries, LB1 and LB2, and water elevations and tangential velocity components at the upper boundaries, UB1 and UB2.

(c) Normal and tangential velocity components at all four open boundaries.

(d) Normal and tangential velocity components along the boundaries LB1, LB2 and UB1, with water elevations being prescribed along UB2.

All four combinations gave similar velocity field predictions within the harbour, with some discrepancies occurring at the open boundaries. Combination (a) yielded the worst flow field predictions at the boundaries, where unrealistic circulation patterns were predicted along the water elevation boundaries, see Mardapitta-Hadjipandeli (12). For combination (b), grid scale oscillations were observed along the boundary UB1 and an obvious poor reproduction of the water elevation field was predicted using combination (c). The best water elevation and velocity field predictions were obtained using combination (d) and hence this inter-connecting boundary combination was used for all of the subsequent numerical model simulations.

Apart from applying the nested model to the idealised rectangular harbours at the laboratory model scale, the model was also applied to the equivalent scaled prototype harbours. The main objective of this exercise was to model directly the physical processes associated with tidal action in such harbours, thus enabling the influence of scaling in the physical model simulations to be considered. The nested model for the prototype harbours was geometrically similar to that for the physical model scale tests. The boundary conditions for the coarse and fine grid models were the same as those deployed in the physical scale model tests, with the exception of the coarse-grid model open boundary, where the

inclusion of the Coriolis term required the inclusion of a water surface slope, see Falconer et al (9). All prototype simulations were commenced from an initial state of rest, at low tide, with a timestep of 60s in the coarse-grid model and 20s in the fine-grid model - again giving rise to a Courant number of 9 in both models. As before, the computations were performed for two complete tidal cycles, with velocity, elevation and concentration fields being reproduced at every quarter of the tidal cycle.

Summary of Results

The complete set of results, for both the mathematical and physical model studies, are described in detail in Mardapitta-Hadjipandeli (12). For the nested numerical model the main finding was that the velocity field within the fine-grid model was best described by transferring only velocity information from the coarse grid model at all but one inter-connecting boundary, and by transferring water elevations at the remaining open boundary. The nested model gave better results than the non-nested model, for a similar computational effort, with the velocity fields predicted by the nested model being in much closer agreement with the physical model results. The coarse and fine grid flow structure was often significantly different between comparable simulations, with the coarse grid model incorrectly predicting a strong eddy at low tide for example. Furthermore the fine grid flow structure within the idealised harbours was not found to be strongly affected by the coarse grid flow structure, with this being best illustrated when the advective accelerations were excluded from the coarse grid model - see Mardapitta-Hadjipandeli (12).

For the laboratory scale model tests, comparisons showed a close agreement between the measured and predicted velocity and concentration distributions, as can be seen for the velocity distributions by comparing Figs. 4 and 6 respectively. An analysis of the results for the free shear and bed generated stress distributions showed that these turbulent stress components were of a similar magnitude at this scale, although from the vorticity field distributions it was confirmed that the effects of bed friction variations were not significant. Comparisons were also undertaken to establish the significance of using free slip and no slip boundary conditions at the closed boundaries, with the results confirming that the flow structure was very different for these two types of boundary condition. The no slip boundary condition gave much closer agreement with the physical model results and it was therefore concluded that this boundary condition was more appropriate in the numerical model, even though the boundary layer thickness was generally a sub-grid scale phenomenon. In terms of the flushing efficiency and exchange characteristics, the numerical and physical model results both indicated that there was a marked reduction in the exchange coefficient for aspect ratios (i.e. L/B ratios) of less than about 0.5 and greater than 2.0. The numerical model results indicated that the peak exchange coefficient occurred for an aspect ratio of unity, i.e. for a square harbour, although this was not clearly confirmed from the physical model results. Finally, for all of the comparisons undertaken at the laboratory model scale, it was evident from both types of modelling procedures that the harbour corners were always observed to be regions of poor local exchange.

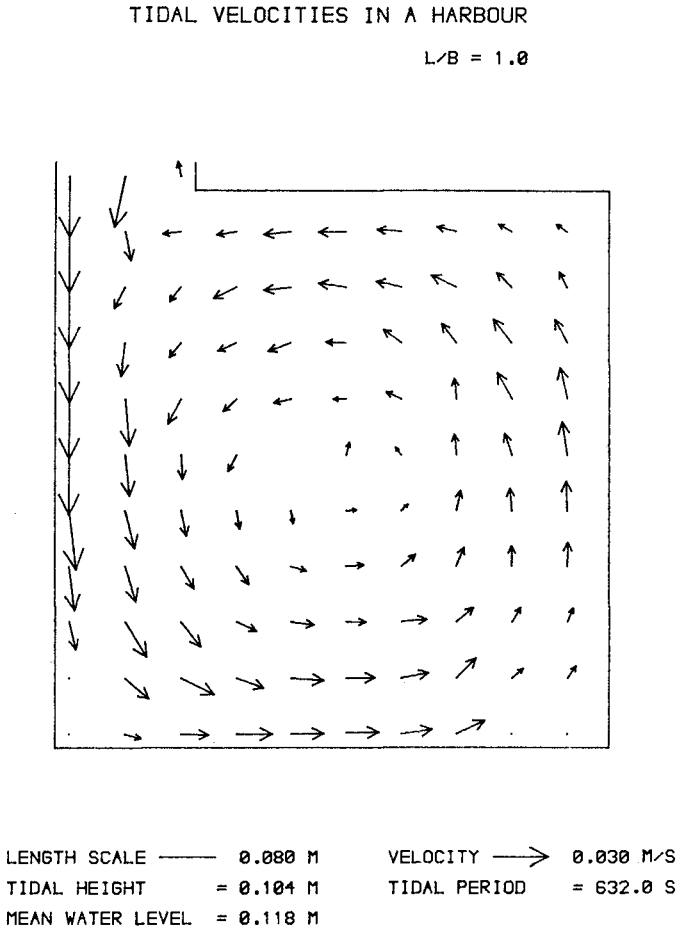


FIG.4 Experimentally Measured Velocities at Mean Water Level Flood Tide for L/B = 1.0

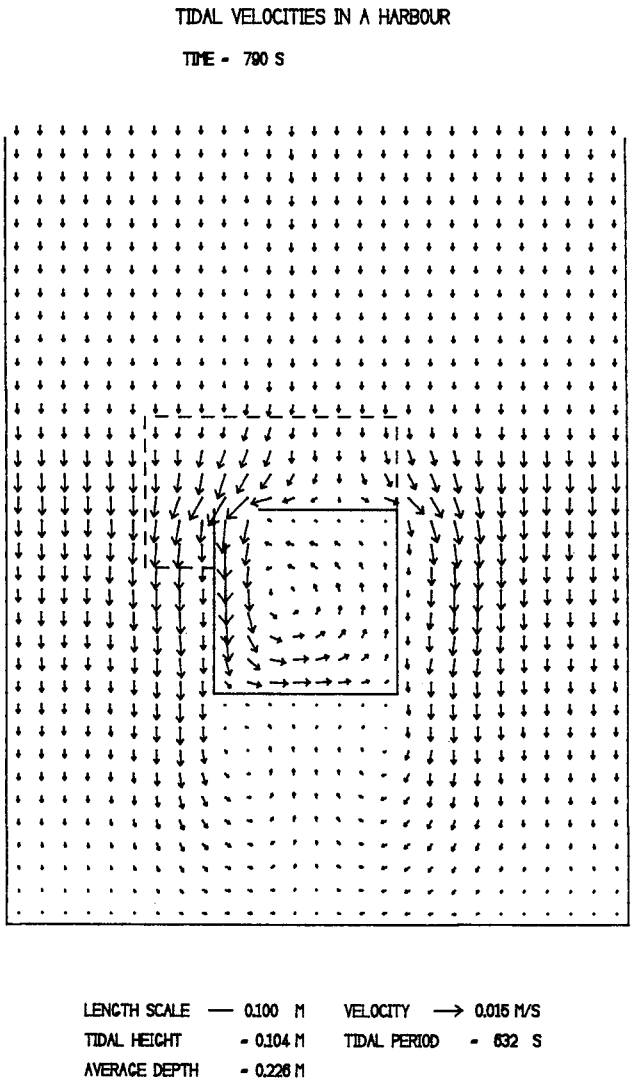


FIG.5 Predicted Coarse-Grid Velocity Field in Model at Mean Water Level Flood Tide for L/B = 1.0

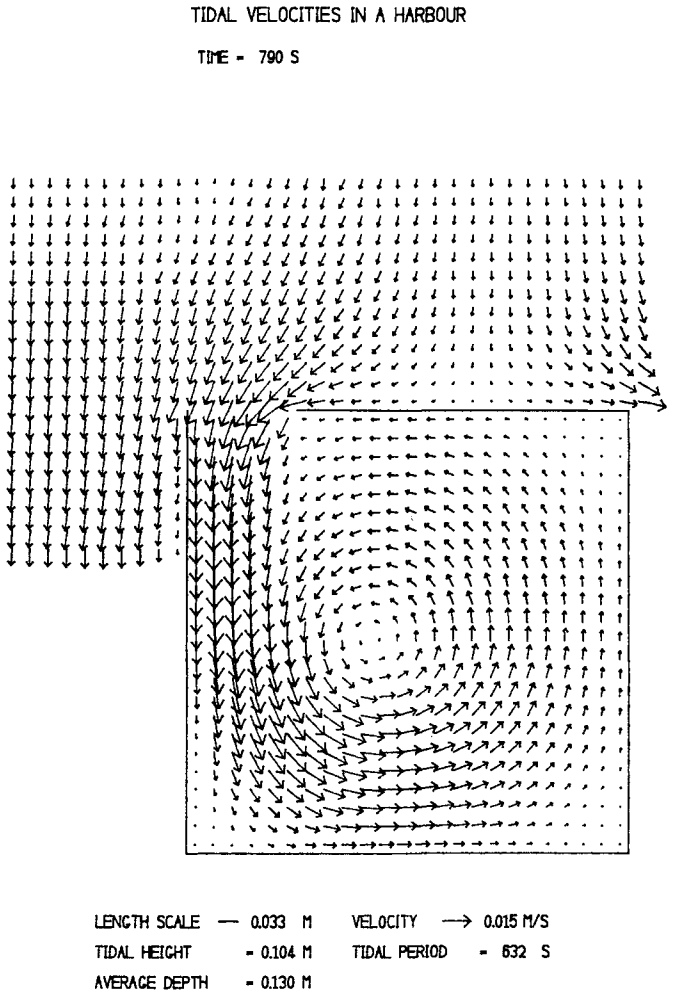


FIG.6 Predicted Fine-Grid Velocity Field in Model at Mean Water level Flood Tide for L/B = 1.0

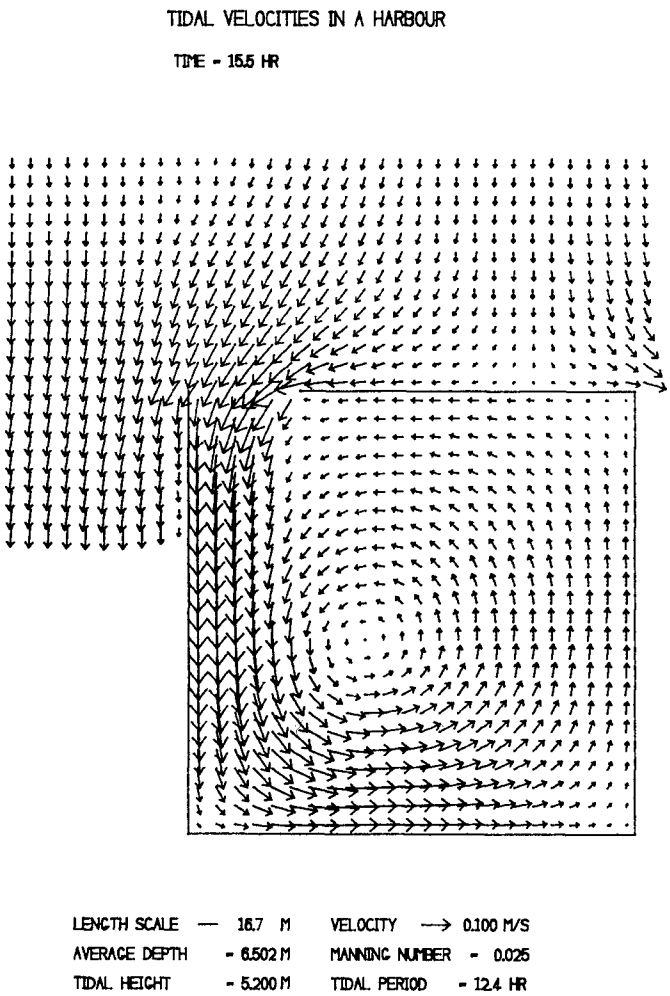


FIG.5 Predicted Fine-Grid Velocity Field in Prototype at Mean Water Level Flood Tide for B/L = 1.0

For the prototype numerical model simulations, comparisons with the laboratory model scale numerical results showed similar agreement for the coarse grid results. However, for the fine grid comparisons the velocity field patterns were often markedly different, see Mardapitta-Hadjipandeli (12). This difference between the prototype and laboratory model scale predictions was particularly pronounced during an ebb tide and was highlighted by the obvious difference in the eddy structure. Such a difference in the numerical model results for the prototype and laboratory model scale harbours has confirmed the problems associated with laboratory model studies of recirculating flows and has raised further questions as to the suitability of distorted laboratory models. As for the laboratory model scale simulations, an analysis was undertaken of the relative magnitudes of the free shear stress and bed generated stress components. The resulting comparisons showed that the free shear stress dominated over the bed generated stress in the mixing zone - unlike the laboratory model scale results - with this conclusion being confirmed by theory (12). Likewise, pronounced changes in the bed roughness coefficient were shown to have a marked effect on the vorticity structure, whereas the effects of dispersion were found to be less significant in the prototype simulations. These results also differed from the laboratory model scale predictions and confirmed the implications of a dimensional analysis study, in that vertical distortion results in an over-estimation of dispersion-diffusion processes and momentum transfer by bed generated turbulence, and an under-estimation of the effects of bed friction. Finally, the numerically predicted prototype scale exchange coefficients and flushing characteristics indicated that the optimum flushing efficiency occurred for an aspect ratio of 2.6, with a distinct reduction occurring in the exchange coefficient for a square harbour. A comparison of the corresponding standard deviation of the concentration distribution within the various shaped harbours, at both prototype and laboratory model scales, also showed that the concentrate was more uniformly mixed in the prototype harbours.

## Conclusions

A nested numerical model has been developed and applied to idealised rectangular harbours to predict velocity fields, exchange coefficients and flushing efficiencies for various harbour shapes. Encouraging agreement has been obtained between the numerical model predictions and laboratory model results at the same scale, with similar prototype model simulations and comparisons highlighting the problems associated with scaling effects in distorted laboratory models. The laboratory model scale results showed that the exchange coefficient deteriorated markedly for rectangular harbours when the length to breadth ratio was less than 0.5 or greater than 2.0, whereas for the prototype model simulations the optimum exchange coefficient was obtained when the aspect ratio was about 2.6.

## Acknowledgements

The mathematical and laboratory model studies reported herein were undertaken at the Department of Civil Engineering, University of Birmingham, with the study being partially funded by the Science and Engineering Research Council.

References

1. Falconer, R.A., "Numerical Modelling of Tidal Circulation in Harbours", Journal of the Waterway, Port, Coastal and Ocean Division, ASCE, Vol.106, No.WW1, February 1980, pp31-48.

2. Falconer, R.A., "A Mathematical Model Study of the Flushing Characteristics of a Shallow Tidal Bay", Proceedings of the Institution of Civil Engineers, Part 2, Vol.77, September 1984, pp.311-332.

3. Falconer, R.A., "Modelling of Planform Influence on Circulation in Harbours", Proceedings of the Seventeenth Coastal Engineering Conference, ASCE, Sydney, Australia, March 1980, pp.2726 - 2744.

4. Jiang, J.X. and Falconer, R.A., "On the Tidal Exchange Characteristics of Model Rectangular Harbours", Proceedings of the Institution of Civil Engineers, Part 2, Vol.75, September 1983, pp.475 - 489.

5. Jiang, J.X. and Falconer, R.A., "The Influence of Entrance Conditions and Longshore Currents on Tidal Flushing and Circulation in Model Rectangular Harbours", International Conference on Numerical and Hydraulic Modelling of Ports and Harbours, BHRA, Birmingham, England, Paper B4, April 1985, pp.65 - 74.

6. Falconer, R.A., "Mathematical Modelling of Jet-Forced Circulation in Reservoirs and Harbours", thesis presented to the University of London, England, in partial fulfillment of the requirements of the degree of Doctor of Philosophy, 1976, pp.237.

7. Dronkers, J.J., "Tidal Computations in Rivers and Coastal Seas", North Holland Publishing Co., Amsterdam, The Netherlands, 1964.

8. Kuipers, J. and Vreugdenhil, C.B., "Calculations of Two-Dimensional Horizontal Flow", Report No.S163, Part 1, Delft Hydraulics Laboratory, Delft, The Netherlands, 1973.

9. Falconer, R.A., Wolanski, E. and Mardapitta-Hadjipandeli, L., "Modelling Tidal Circulation in an Island's Wake", Journal of Waterway, Port, Coastal and Ocean Engineering, Vol.121, No.2, March 1986, pp.234-254.

10. Falconer, R.A. and Mardapitta-Hadjipandeli, L., "Bathymetric and Shear Stress Effects on an Island's Wake: A Computational Model Study", Coastal Engineering (in press).

11. Fisher, H.B., "On the Tensor Form of the Bulk Dispersion Coefficient in a Bounded Skewed Shear Flow", Journal of Geophysical Research, Vol.83, No.C5, May 1978, pp.2373-2375.

12. Mardapitta-Hadjipandeli, L. "Numerical Modelling of Tidal Circulation", thesis presented to the University of Birmingham, England, in partial fulfillment of the requirements for the degree of Doctor of Philosophy, 1985, pp.293.

13. Leendertse, J.J., "A Water-Quality Simulation Model for Well-Mixed Estuaries and Coastal Seas : Vol.1, Principles of Computation", The Rand Corporation, RM-6230-RC, February 1970, pp.70.

14. Falconer, R.A., "Temperature Distributions in a Tidal Flow Field", Journal of Environmental Engineering, ASCE, Vol.110 No.6, December 1984, pp.1099-1116.

15. Nece, R.E. and Richey, E.P., "Flushing Characteristics of Small Boat Marinas", Proceedings of the Thirteenth Coastal Engineering Conference, ASCE, Vancouver, 1972, pp.2499-2512.

16. Thabet, R.A.H., Verboom, G.K. and Akkerman, G.J., "Two-Dimensional Modelling of Tidal Motion for Harbour Studies", Proceedings of the International Conference on Numerical Modelling of Ports and Harbours, BHRA Birmingham, England, April 1985, pp.23-32.